Title
Dominant Mutations in GRHL3 Cause Van der Woude Syndrome and Disrupt Oral Periderm Development

Journal
American Journal of Human Genetics, 94(1)

ISSN
0002-9297

Authors
Peyrard-Janvid, Myriam
Leslie, Elizabeth J
Kousa, Youssef A
et al.

Publication Date
2014

DOI
10.1016/j.ajhg.2013.11.009

Peer reviewed

Dominant Mutations in *GRHL3* Cause Van der Woude Syndrome and Disrupt Oral Periderm Development

Myriam Peyrard-Janvid,[1,16,*] Elizabeth J. Leslie,[2,16] Youssef A. Kousa,[3,16] Tiffany L. Smith,[4,16] Martine Dunnwald,[2,16] Måns Magnusson,[5] Brian A. Lentz,[2] Per Unneberg,[6] Ingegerd Fransson,[1] Hannele K. Koillinen,[7] Jorma Rautio,[8] Marie Pegelow,[9] Agneta Karsten,[9] Lina Basel-Vanagaite,[10,11,12] William Gordon,[13] Bogi Andersen,[13] Thomas Svensson,[5] Jeffrey C. Murray,[2] Robert A. Cornell,[4] Juha Kere,[1,5,14,*] and Brian C. Schutte[15]

Mutations in interferon regulatory factor 6 (*IRF6*) account for ~70% of cases of Van der Woude syndrome (VWS), the most common syndromic form of cleft lip and palate. In 8 of 45 VWS-affected families lacking a mutation in *IRF6*, we found coding mutations in grainyhead-like 3 (*GRHL3*). According to a zebrafish-based assay, the disease-associated *GRHL3* mutations abrogated periderm development and were consistent with a dominant-negative effect, in contrast to haploinsufficiency seen in most VWS cases caused by *IRF6* mutations. In mouse, all embryos lacking *Grhl3* exhibited abnormal oral periderm and 17% developed a cleft palate. Analysis of the oral phenotype of double heterozygote ($Irf6^{+/-}$;$Grhl3^{+/-}$) murine embryos failed to detect epistasis between the two genes, suggesting that they function in separate but convergent pathways during palatogenesis. Taken together, our data demonstrated that mutations in two genes, *IRF6* and *GRHL3*, can lead to nearly identical phenotypes of orofacial cleft. They supported the hypotheses that both genes are essential for the presence of a functional oral periderm and that failure of this process contributes to VWS.

Introduction

Grainyhead-like 3 (*Drosophila*) (*GRHL3* [MIM 608317]) belongs to a family of three human genes that encode transcription factor orthologs of the *Drosophila* gene *grainy head* (*grh*). Among multiple conserved roles, this gene family is required for the development and repair of the epidermal barrier layer.[1–3] In zebrafish, *grhl1* and *grhl3* were shown to be required for the development of the periderm,[4] the transient layer of squamous epithelial cells located on the surface of developing embryos. Interferon regulatory factor 6 (*irf6*) is also required for periderm development in zebrafish[5] and directly regulates the expression of *grhl3*.[4,6] In addition, overexpression of *Grhl3* partially rescued periderm development in zebrafish embryos that expressed a dominant-negative mutant form of *irf6*.[4] These data suggest that *Grhl3* is an important player in the *Irf6*-dependent pathway of periderm development.

IRF6 belongs to the IRF family of transcription factors that are known best for their roles in immune function.[7] However, *IRF6* (MIM 607199) is required for skin, limb, and craniofacial development.[8–10] In mice, embryos that lack *Irf6* expression fail to develop the epidermal barrier.[9,10] Although reminiscent of embryos that lack *Grhl3*,[2] the cutaneous phenotype of *Irf6* mutant embryos appears to be more severe macroscopically. In addition, *Irf6* mutant embryos have extensive oral epithelial adhesions,[9,10] a phenotype not reported in the *Grhl3* mutant. The oral epithelial adhesions in *Irf6* knockout embryos lead to cleft palate[9,10] and appear to stem from periderm dysfunction.[4,11]

In humans, mutations in *IRF6* cause Van der Woude syndrome (VWS [MIM 119300]), the most common syndromic form of orofacial clefting, or popliteal pterygium syndrome (PPS [MIM 119500]). Individuals with VWS can have cleft lip (CL), cleft palate (CP), or cleft lip and palate (CLP). In addition, 85% of affected individuals have pits in their lower lip.[12] To date, mutations in *IRF6* have been identified in 70% of families with VWS.[8,13,14] The possibility that locus heterogeneity accounts for some of the remaining 30% of VWS mutations is underscored by linkage in one large pedigree from Finland to a locus on 1p33–p36 rather than to *IRF6* at 1q32–q41.[15] In this family, most affected individuals have an orofacial cleft and

[1]Department of Biosciences and Nutrition, Karolinska Institutet, and Center for Biotechnology, 14183 Huddinge, Sweden; [2]Department of Pediatrics and Interdisciplinary Program in Genetics, University of Iowa, Iowa City, IA 52242, USA; [3]Department of Biochemistry and Molecular Biology, Michigan State University, East Lansing, MI 48824, USA; [4]Department of Anatomy and Cell Biology, University of Iowa, Iowa City, IA 52242, USA; [5]Department of Biosciences and Nutrition, Science for Life Laboratory, Karolinska Institutet, 17121 Solna, Sweden; [6]Department of Biochemistry and Biophysics Science for Life Laboratory, Stockholm University, 17121 Solna, Sweden; [7]Department of Clinical Genetics, Helsinki University Hospital, 00029 Helsinki, Finland; [8]Cleft Palate and Craniofacial Center, Department of Plastic Surgery, Helsinki University Hospital, 00029 Helsinki, Finland; [9]Department of Orthodontics, Stockholm Craniofacial Team, Institute of Odontology, Karolinska Institutet, 17177 Stockholm, Sweden; [10]Pediatric Genetics Unit, Schneider Children's Medical Center of Israel and Raphael Recanati Genetic Institute, Rabin Medical Center, Petah Tikva 49100, Israel; [11]Sackler Faculty of Medicine, Tel Aviv University, Tel Aviv 69978, Israel; [12]Felsenstein Medical Research Center, Petah Tikva 49100, Israel; [13]Department of Biological Chemistry, University of California Irvine, Irvine, CA 92697, USA; [14]Research Programs Unit, University of Helsinki, and Folkhälsan Institute of Genetics, 00014 Helsinki, Finland; [15]Department of Microbiology and Molecular Genetics, Michigan State University, East Lansing, MI 48824, USA
[16]These authors contributed equally to this work
*Correspondence: myriam.peyrard@ki.se (M.P.-J.), juha.kere@ki.se (J.K.)
http://dx.doi.org/10.1016/j.ajhg.2013.11.009.

the proband has lip pits, the hallmark of VWS. Because of the autosomal-dominant inheritance pattern and the presence of the lip pits, this family was diagnosed with VWS and the linked region was named the *VWS2* locus.[15]

Here we report disease-causing mutations in *GRHL3* in the above-mentioned original Finnish family as well as in seven additional families with VWS, thereby demonstrating that *GRHL3* is the second gene for which mutations lead to VWS. Although we observed no consistently unique phenotypes in these families, individuals with a *GRHL3* mutation are more likely to have CP and less likely to have CL or lip pits than individuals with an *IRF6* mutation. In addition, we used zebrafish and murine models to show that *Grhl3*, like *Irf6,* has a conserved role in the development of the periderm. Our observations from all three species support the conclusion that a functional oral periderm is essential for the proper palatogenesis.

Material and Methods

Human DNA Samples

DNA samples from 45 families of multiple ethnicities and who were completely sequenced for *IRF6* without identifying a causative mutation were used in this study. All subjects were examined by clinical geneticists or genetic counselors who made diagnoses as described previously.[15–17] Written informed consent was obtained for all subjects and all protocols were approved by the local ethical boards in Helsinki (Finland) or in Stockholm (Sweden) or by the Institutional Review Boards at the University of Iowa (USA). A total of 360 unrelated individuals without a history of oral cleft from the Philippines were used as controls for the *GRHL3* (c.1171C>T) Filipino variant and 561 unrelated Finnish individuals (blood donors) were used as controls for the *GRHL3* (c.969_970insTG), the *PHACTR4* (c.1615G>A; rs200581707), and the *KTI12* (c.337_363delCCGATCGCGGGACCTCAGGTGG CGGGC; ss836732090) Finnish variants.

Targeted Exome Sequencing

Genomic DNA from eight affected and three healthy individuals from the *VWS2* Finnish family underwent SureSelect Target Enrichment (Agilent Technologies) in order to perform sequence capture of the exome. Enriched samples were sequenced on an Illumina HiSeq instrument. Reads were aligned to reference sequence with the bwa read mapper.[18] A high-quality variant call set was generated based on a best-practice workflow,[19] in which we utilized the Picard and Genome analysis toolkit (GATK) for data processing and analysis.

Genotyping

Genotyping of the *GRHL3* c.969_970insTG (Finnish) and c.1171C>T (Filippino) variants and the *PHACTR4* (c.1615G>A; rs200581707) Finnish variant was performed with TaqMan SNP Genotyping Assays (Life Technologies) on the ABI Prism 7900HT or ABI 7500 and analyzed with SDS 2.3 or SDS 1.4 software (Applied Biosystems). Family relationships for apparently de novo variants (c.1171C>T and c.1559_1562delGGAG) were confirmed by genotyping 16 markers distributed across the genome (Table S2 available online). The *KTI12* (c.337_363delCC GATCGCGGGACCTCAGGTGGCGGGC; ss836732090) variant was genotyped by PCR amplification with SYBR green labeling of the wild-type (100 bp) and the deleted (73 bp) alleles and checked for their respective melting temperatures/curves.

Mutation Screening by Sanger Sequencing

Primers for *GRHL3* were designed to amplify the exons of all isoforms of *GRHL3* via Primer3. The exons of all four *GRHL3* transcript variants were screened in a total of 13 PCR amplicons (Table S1). PCR reactions were incubated at 94°C for 5 min followed by 35 amplification cycles (45 s at 94°C, 45 s at 60°C, 45 s at 72°C) and a final extension at 72°C for 7 min. PCR products were sent for sequencing on an ABI 3730XL (Functional Biosciences). Chromatograms were transferred to a UNIX workstation, base-called with PHRED (v.0.961028), assembled with PHRAP (v.0.960731), scanned by POLYPHRED (v.0.970312), and viewed with the CONSED program (v.4.0). The effects of missense variants were predicted with the Variant Effect Predictor program,[20] which generates scores from PolyPhen2 and SIFT.

Phenotype Analysis

Affected individuals with *GRHL3* mutations (n = 27) were assigned a phenotype classification of cleft lip with or without cleft palate (CL/P includes CL and CLP cases), cleft palate (CP), lip pits only, CL/P with lip pits, or CP with lip pits based on the clinical diagnoses. Additional phenotypic classifications described the presence of dental anomalies (hypodontia, dental aplasia, or malocclusion), limb anomalies (syndactyly, polydactyly, club foot, or contractures), or popliteal pterygia. From the set of families positive for *IRF6* mutations,[8,13,14,17,21] affected individuals were also assigned to the same phenotype classifications (n = 632). Exclusion criteria for this analysis were individuals with a cleft but without identified familial mutation (i.e., potential phenocopies) and individuals diagnosed with VWS without a known *IRF6* or *GRHL3* mutation.

Transfection of Human *GRHL3* Mutation Variants into Zebrafish Embryos

Full-length, wild-type human *GRHL3* cDNA variant 4 (v4) was obtained as a cDNA clone from Open Biosystems (MHS1010-9204655) and shuttled by Gateway cloning into the CS2+ destination vector (kindly provided by Dave Turner, University of Michigan). This construct was used for in vitro synthesis of wild-type *GRHL3* mRNA. Specific mutations from VWS-affected individuals were generated in the *GRHL3* mRNA (v4) via PCR-mediated mutagenesis and the resulting cDNAs engineered into CS2+, resulting in the truncation of the first 6 bp of 5′ UTR and the last 70 bp of 3′ UTR from mutant variants. These constructs were further used for in vitro synthesis of mutant variants of *GRHL3*. These truncations (the first 6 bp of 5′ UTR and the last 70 bp of 3′ UTR from mutant variants) had no functional consequence, as shown by the fact that we tested a similarly truncated and cloned wild-type *GRHL3*, and *GRHL3* mRNA synthesized from this construct behaved equivalently to full-length *GRHL3* in the zebrafish-based functional assay.

Capped mRNA was synthesized in vitro (mMESSAGE mMACHINE SP6 kit, Ambion) and purified with the MEGAclear kit (Ambion) and approximately 1 ng of mRNA was injected into wild-type zebrafish embryos (Scientific Hatcheries outbred strain) at the 1-cell or, for mosaic injections, at the 16-cell stage. Embryos were fixed at 50% epiboly or corresponding time-point (5–6 hpf), and whole-mount in situ hybridization for *krt4* was performed as

previously described.[22] Plasmids used for probe synthesis are available upon request. Embryos were injected with biotinylated-dextran (Invitrogen, D-1956) and processed for visualization as previously described.[4] Animal use protocols were approved by the Public Health Service Assurance.

Murine Crosses

We crossed mice heterozygous for the *Irf6* genetrap allele ($Irf6^{+/gt}$; here referred to as $Irf6^{+/-}$)[9] with mice heterozygous for the *Grhl3* knockout allele ($Grhl3^{+/-}$)[3] to generate wild-type, $Irf6^{+/-}$, $Grhl3^{+/-}$, and $Irf6^{+/-}$;$Grhl3^{+/-}$ double heterozygous embryos. *Grhl3* knockout embryos were obtained by crossing $Grhl3^{+/-}$ mice. Presence of a copulation plug was denoted as E0.5. Pregnant dams were injected intraperitoneally with BrdU (Sigma) 2 hr before euthanization at a dose of 100 μg per gram pregnant dam body weight. Embryos were collected at indicated time points and genotyped for *Irf6* and *Grhl3* null alleles as described previously.[3,9] Both alleles were maintained on a C57BL/6 background. Animal use protocols were approved by the Institutional Animal Care and Use Committees at Michigan State University and the University of California, Irvine.

Morphological, Histological, and Molecular Analyses of Mice

Gross morphological analysis of the $Irf6^{+/-}$ by $Grhl3^{+/-}$ cross was done at E13.5, E17.5, P0, and P21. Embryos were then fixed in 4% paraformaldehyde, embedded in paraffin, and sectioned at 7 μm intervals. Haematoxylin and eosin staining was performed as described.[9] For immunostaining, antigen retrieval was performed in sodium citrate, followed by blocking steps in BSA and a goat anti-mouse Fab fragment (Jackson ImmunoResearch Laboratories, 115-007-003). Primary antibody was incubated overnight at 4°C and secondary antibody was incubated for 1.5 hr at room temperature. We used primary antibodies against Keratin 6 (Covance, PRB-190 169P), tumor protein p63 (Santa Cruz, 4A4, SC-8431), Irf6 (Sigma-Aldrich, SAB2102995), and Activated Notch1 (Act N1, Cell Signaling, Val1744, D3B8, 4147S). We used the following secondary antibodies: goat anti-rabbit (Molecular Probes, A21429), goat anti-mouse (Molecular Probes, A11029), and goat anti-rat (Molecular Probes, A11006). Nuclei were stained with DAPI (Invitrogen, D3571) followed by slide mounting in ProLong Gold Antifade Reagent (Invitrogen, P36930).

Imaging

Histological and immunostained sections were imaged with a Nikon Eclipse 90i upright microscope with a Plan APO 10×/0.45 DIC, a CFI Plan Apo Lambda 20×/0.75, and a Plan APO 40×/0.95 DIX M/N2 objectives. A Nikon DS-Fi1 high-definition camera head and a DigitalSight PC-use control unit were used for haematoxylin and eosin imaging. A X-Cite Series 120Q laser and a CoolSnap HQ2 photometric camera were used to obtain immunofluorescent images. NIS Elements Advanced Research v.3.10 was used for RAW image deconvolution and Adobe Photoshop Elements v.9.0 was used for figure formation.

Statistical Analysis

Fisher's exact test in STATA (v.12.1) was used to compare the frequencies of VWS-associated phenotypes between individuals with *GRHL3* mutations and those with *IRF6* mutations. The threshold p value for this analysis was calculated with a Bonferroni correction ($p = 0.05$; 8 phenotypes = 0.006). We used chi-square analysis to compare the observed genotype distributions of mice with the predicted Mendelian frequencies. Previous reports show that resorption rates in C57BL/6 mice range between 1% and 3%. We used a two-tailed Fisher's exact test to compare the upper limit of this range with the observed resorption rates.

Results

GRHL3 Is the *VWS2* Gene

A single large VWS-affected family of Finnish origin (Figure S1) showed linkage to a ~40 cM region on 1p33–36, pointing to a second VWS locus,[15] i.e., *VWS2* (MIM 606713). From this family, we selected eight affected individuals, including the proband who is the only one with lip pits, and three healthy individuals for whole-exome sequencing. We searched the ~700 genes contained in the entire linkage region (~46 Mb) for variants common to all eight affected family members but not seen in any of the three healthy members. This resulted in three segregating exonic variants in *GRHL3* (chr1: 24,666,175; RefSeq accession number NM_198174.2; c.969_970insTG), *PHACTR4* (chr1: 28,806,971; rs200581707; RefSeq NM_001048183.1; c.1615G>A), and *KTI12* (chr1: 52,499,097–52,499,071; ss836732090; RefSeq NM_138417.2; c.337_363delCCGA TCGCGGGACCTCAGGTGGCGGGC). The *GRHL3* and *PHACTR4* variants were confirmed by TaqMan genotyping and the *KTI12* variant by allelic discrimination based on differential melting temperature. The *PHACTR4* variant was found in 2 out of 8,252 European American chromosomes in the NHLBI/ESP database and is therefore unlikely to be the causative variant for VWS. In a set of 561 Finnish controls, the *KTI12* variant was found at a frequency of 12.4% and is therefore a common, noncausative variant. The *GRHL3* variant was not found in any of the Finnish controls nor in NHLBI/ESP, making *GRHL3* a strong candidate gene in the *VWS2* locus.

To test whether mutations in *GRHL3* accounted for VWS in other families, we screened 44 families of variable ethnicity where no causative *IRF6* mutations had been previously detected. We identified *GRHL3* variants in seven families, including four protein-truncating mutations and four missense mutations (Figure 1). All mutations except c.1661A>G (coding for the p.Asn554Ser missense alteration) were predicted by PolyPhen2 and SIFT to be damaging/deleterious and two were confirmed de novo events (Table 1). In one of the seven families (VWS-III), we found two variants located in *trans*. Variant c.268_278delTACTACCATGG was inherited from the proband's affected father and from the healthy paternal grandfather, and variant c.1661A>G was inherited from the proband's healthy mother (Figure S1). In addition, one family (VWS-IV) was previously determined to have a novel *IRF6* missense variant (c.239A>G) that was not conclusively determined to be causative for VWS,[23] raising the possibility that variants in both *IRF6* and *GRHL3* could contribute to VWS in one family (Figure S1).

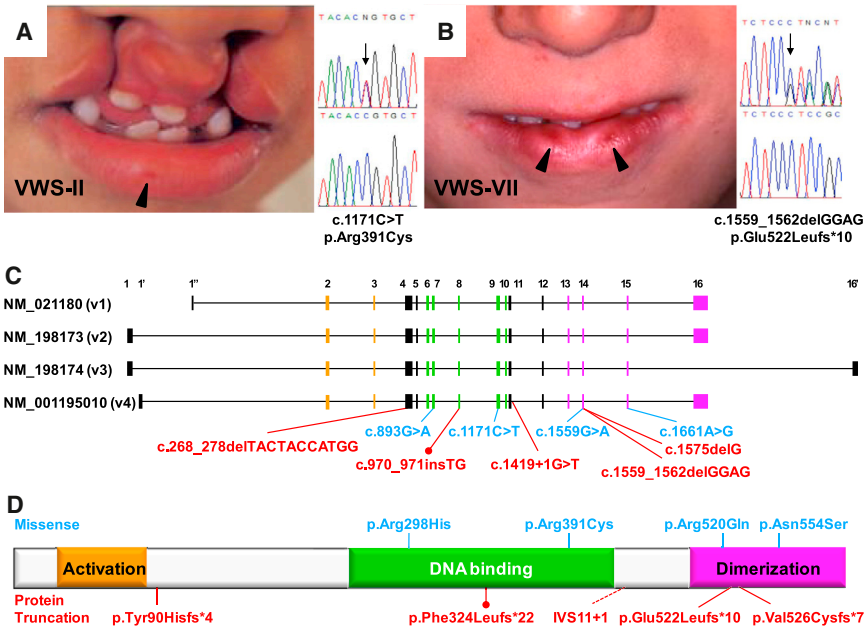

Figure 1. Mutations in *GRHL3* Cause Van der Woude Syndrome

(A and B) Clinical images of the probands from families VWS-II (A) and VWS-VII (B) display the cardinal feature of VWS, i.e., lip pits (arrowhead). Sequence tracks from each individual are shown to the right with an arrow pointing to the base affected by the mutation. Note that the sequence for c.1559_1562delGGAG is to be read from the reverse strand.

(C) *GRHL3* has four alternative transcripts variants, v1 to v4 (UCSC Genome Browser), with three alternative first exons (1, 1′, and 1″) and two alternative last exons (16 and 16′). Translation starts in the first exon of each variant (except for v4 where translation starts in exon 2) and stops in the last exon of each variant. The genomic location and cDNA change of each of the nine mutations observed are indicated (according to v3, RefSeq NM_198174.2). The mutation found in the original Finnish family (VWS-I) is indicated by a filled circle. Colors for the exons are corresponding to their coding for the GRHL3 protein domains.

(D) Schematic representation of the *GRHL3* protein product v2 (RefSeq NP_937816) with (at scale) the three known protein domains: the transactivation (orange), the DNA binding (green), and the dimerization (pink) domains. The position of each change in the protein sequence is also indicated. Please note that because no mutation was found in exon 16, the denomination for each amino acid change is valid both in v2 and v3. More details of the v2 full protein sequence can also be found in Figure S2.

We tested for phenotypic variation between the *VWS* and *VWS2* loci. The phenotypes observed in the individuals with mutations in *GRHL3* overlap with the classic VWS phenotype (Figure S1). However, individuals positive for a *GRHL3* mutation were significantly more likely to have CP (70% [*GRHL3*] versus 27% [*IRF6*], p value = 2.0×10^{-6}) and less likely to have CL/P (CL or CLP) (11% versus 46%, p value = 0.001) than individuals with *IRF6* mutations (Table 2). Lip pits were less frequent among individuals with *GRHL3* mutations (52% versus 76%), but this difference was not statistically significant (p value = 0.05). The presence of dental and limb anomalies did not differ significantly between the two groups.

Effect of *GRHL3* Alleles on Zebrafish Development

To distinguish whether the human *GRHL3* alleles that cause VWS are nulls or dominant negative, we developed an in vivo assay to measure the function of the gene on

Table 1. *GRHL3* Mutations in Eight Van der Woude Syndrome-Affected Families

VWS Pedigree	Origin	DNA Change[a]	Protein Change[b]	Genomic Position[c]	Exon	De Novo/ Familial
I[d]	Finland	c.970_971insTG	p.Phe324Leufs*22	chr1: 24,666,175	8	familial
II	Philippines	c.1171C>T	p.Arg391Cys[e]	chr1: 24,668,728	9	de novo
III	Israel	c.[268_278delTACTAC CATGG];[1661A>G][f]	p.[Tyr90Hisfs*4]; [Asn554Ser][f]	chr1: 24,662,973–24,662,983; 24,676,579	4; 15	familial
IV	Pakistan	c.893G>A	p.Arg298His[e]	chr1: 24,664,534	7	NA
V	UK	c.1419+1G>T	splice donor site; IVS11+1	chr1: 24,669,516		familial
VI	USA	c.1559G>A	p.Arg520Gln[e]	chr1: 24,673,973	14	NA
VII	Sweden	c.1559_1562delGGAG	p.Glu522Leufs*10	chr1: 24,673,973–24,673,976	14	de novo
VIII	USA (African American)	c.1575delG	p.Val526Cysfs*7	chr1: 24,673,989	14	familial

Abbreviation is as follows: NA, not applicable because parent DNA was unavailable.
[a]Position on *GRHL3* cDNA variant 3 (v3) RefSeq NM_198174.2.
[b]Position on *GRHL3* protein product RefSeq NP_937817.3.
[c]Position according to the UCSC Genome Browser human genome reference hg19.
[d]Family studied originally by linkage analysis in Koillinen et al.[15] and here by exome sequencing.
[e]Missense mutation predicted to be damaging by PolyPhen2 and SIFT by the Variant Effect Predictor program.
[f]Mutations occurring in the same family but on separate chromosomes as indicated.

Table 2. Comparison of VWS Phenotypes Caused by Mutations in *IRF6* and *GRHL3*

Has Phenotype?	CL/P[a]	CP	Cleft Only[b]	Lip Pits	Lip Pits Only	Dental Anomalies[c]	Limb Defects[d]	Pterygia[e]
***GRHL3* (n = 27)**								
yes	3	19	12	14	5	2	2	0
no	24	8	15	13	22	25	25	27
%	11	70	44	52	19	7	7	0
***IRF6* (n = 632)**								
yes	267	159	141	445	158	70	45	10
no	365	473	491	187	474	562	587	622
%	46	27	24	76	27	12	8	2
p value	0.001	2.0×10^{-6}	0.02	0.05	0.65	0.76	1	1

[a]Includes cleft lip (CL) and cleft lip and palate (CLP).
[b]Includes cleft palate (CP), CL, or CLP but without lip pits.
[c]Dental anomalies include hypodontia, dental aplasia, and malocclusion.
[d]Includes syndactyly, polydactyly, club foot, contractures, and pterygium.
[e]Only pterygia counted.

the development of the periderm in zebrafish.[4] The assay is based on the observation that overexpression of wild-type *grhl3* in zebrafish or frog embryos (*Xenopus laevis*) is sufficient to induce, in deep cells, ectopic expression of genes whose expression is normally restricted to the periderm, e.g., *keratin 4* (*krt4*).[4,24] Also, simultaneous reduction of *grhl1* and *grhl3*, or overexpression of an engineered dominant-negative variant of frog *grhl1*, prevents the expression of *krt4* in epithelial cells of the zebrafish periderm and causes embryonic death during epiboly.[4]

Therefore, we injected wild-type and mutant alleles of human *GRHL3* mRNA into zebrafish embryos and scored for embryonic viability and *krt4* expression. At shield stage (6 hr postfertilization, hpf), most embryos injected with a control mRNA (*lacZ*) developed normally, and *krt4* expression was confined to the periderm (Figures 2A and 2E). In most embryos injected with wild-type *GRHL3*, epiboly was slightly delayed in comparison to *lacZ*-injected control embryos (Figure 2B) and *krt4* was ectopically expressed in deep cells (Figure 2F). In contrast, the majority of embryos injected with *GRHL3* mRNA carrying the c.1171C>T variant from VWS-II stalled before (4 hpf) or during epiboly stage, and then ruptured through the animal hemisphere (Figure 2C). This phenotype resembles that of embryos injected with the dominant-negative alleles of *Xenopus grhl1* or zebrafish *irf6*.[4,5] We tested four other VWS-associated alleles of *GRHL3* with this in vivo assay, including both alleles found in VWS-III. For all four alleles, embryonic development stalled and the embryo ruptured at a time point and frequency similar to embryos injected with the c.1171C>T variant from VWS-II (Figure 2D).

To test whether the effect of these mutations was cell autonomous, we generated mosaic embryos by coinjecting *GRHL3* mRNA and biotin into one cell at the 16-cell stage of zebrafish development. In this assay, cells that inherited the *GRHL3* mRNA were marked by biotin staining. In embryos injected with control mRNA (*LacZ*), we observed normal *krt4* expression in all periderm cells, regardless of the biotin staining (Figure 2G). In embryos injected with *GRHL3* mRNA containing the c.893G>A variant (from VWS-IV), the cells from the periderm inheriting the mutated mRNA (biotin-positive) lacked *krt4* expression, but biotin-negative cells expressed *krt4* (Figure 2H). We conclude that mutant *GRHL3* variant interfered with the development of the periderm in a cell-autonomous fashion. In summary, each of the five *GRHL3* mutations appeared to encode a protein with dominant-inhibitory effect that disrupted the development of the periderm through a cell-autonomous mechanism.

Grhl3$^{-/-}$ Murine Embryos Have Cleft Palate at Low Penetrance

To identify a potential common mechanism for orofacial clefts in individuals with VWS, we compared the oral phenotype of murine embryos that lack *Irf6* (*Irf6*$^{-/-}$) to embryos that lack *Grhl3* (*Grhl3*$^{-/-}$). Wild-type embryos at E15.5 had normal oral epithelium and a fully fused palate (Figure 3A), whereas *Irf6*$^{-/-}$ embryos (n = 4) had extensive epithelial adhesions between the palatal shelves and the lingual, mandibular, and maxillary surfaces (Figure 3B).[9,10] These adhesions prevented the palatal shelves from elevating and led to a cleft palate in all embryos. Similarly, all *Grhl3*$^{-/-}$ embryos at E15.5 had bilateral oral epithelial adhesions (n = 6) and one of these embryos had a cleft palate (Figure 3C). Thus, *Grhl3*, like *Irf6*, is required for palatal development.

To compare the histological changes in these two mutant strains, we immunostained with keratin 6 (Krt6), a marker for the periderm,[25] and tumor protein p63 (p63), a marker for the basal epithelial layer.[26] We detected Krt6 in the oral periderm of wild-type embryos (Figure 3D), but Krt6 expression was strongly reduced in the epithelium superficial to the tooth germs in both *Irf6*$^{-/-}$ and *Grhl3*$^{-/-}$ mutant embryos (Figures 3E and 3F). Similar results were observed for activated Notch1 (Act N1) (Figure S3), another

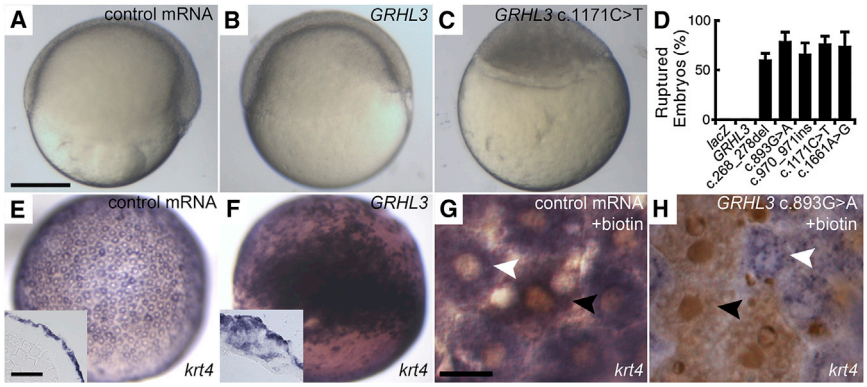

Figure 2. VWS-Associated Alleles of *GRHL3* Disrupt the Development of the Periderm when Expressed in Zebrafish Embryos

(A–C) Lateral views of live sibling embryos injected with control (A), *GRHL3* (B), or *GRHL3* (c.1171C>T) (C) mRNA. Embryo shown in (C), injected with the *GRHL3* mRNA carrying the c.1171C>T mutation, ruptured through the animal hemisphere shortly after the image was taken (67% [n = 48] of wild-type *GRHL3*-injected embryos reached at least 50% epiboly stage, whereas 76% [n = 115] of mutant-injected embryos burst without initiating epiboly). (D) Histogram showing fraction of embryos that ruptured when injected with indicated mRNA. Percentage is the average from 3–4 separate experiments of 20–40 embryos each. Error bars represent standard error.

(E and F) Animal pole views of embryos injected with indicated mRNA and processed to detect *krt4* expression. Insets, cross sections of the same embryos showing (E) *krt4* expression confined to the periderm and (F) ectopically in deep cells.

(G and H) Animal pole views of mosaic embryos injected with mRNA and biotinylated-dextran at 16-cell stage, fixed at shield stage, and processed for *krt4* expression (blue) and biotin distribution (brown). Periderm cells possessed (black arrowhead) or lacked (white arrowhead) biotin stain, demonstrating that they were, or were not, derived from an RNA-injected cell, respectively. Daughter cells derived from the cell injected with the c.893G>A mutant variant of *GRHL3* lack *krt4* expression.

Scale bars represent 500 μm (A–C, E, F), 100 μm (inset in E and F), and 20 μm (G, H).

protein expressed in the periderm.[11] Thus, we concluded that both *Irf6* and *Grhl3* were required for proper development of the oral periderm in the mouse.

In addition to its potential role in the periderm, *Irf6* regulates the differentiation of the keratinocytes in the epidermis[9,10] and the oral cavity.[11] In the oral cavity, wild-type embryos had a uniform, single layer of basal epithelium (Figure 3D), whereas the basal layer in $Irf6^{-/-}$ embryos was disorganized and thicker, and p63 was ectopically expressed in the cells of the suprabasal layer (Figure 3E). In $Grhl3^{-/-}$ embryos, the basal epithelial layer appeared grossly normal with normal expression of p63 (Figure 3F). We also looked at the medial edge epithelium (MEE), the epithelium located at the medial edge of the palatal shelves that must dissolve for proper palatal fusion. In wild-type (Figure 3G) and $Grhl3^{-/-}$ (Figure 3I) embryos, the MEE dissolved to form a confluent bridge of mesenchymal cells across the palate as shown by the loss of expression of p63. In contrast, although we do not know the exact location of the MEE in $Irf6^{-/-}$ embryos, expression of p63 persisted throughout the epithelium of the palatal shelves (Figure 3H).[11] Thus, $Irf6^{-/-}$ embryos have at least two problems during palatal development: the presence of oral epithelial adhesions and the failure of the MEE to dissolve. In contrast, $Grhl3^{-/-}$ embryos have only oral epithelial adhesions because of the loss of periderm. Because mutations in both these genes cause VWS, these results are consistent with the hypothesis that abnormal periderm function contributes to CL/P in humans.

The Oral Phenotypes of *Irf6* and *Grhl3* Heterozygous Murine Mutants Are Independent

Based on ChIP-seq experiments on a human keratinocyte cell line and epistasis experiments in zebrafish embryos, we hypothesized that *Irf6* and *Grhl3* function in a common pathway.[4,6] To test for epistasis during murine palatogenesis, we generated embryos that were heterozygous for both *Irf6* and *Grhl3* ($Irf6^{+/-}$;$Grhl3^{+/-}$). As expected, we did not observe any oral epithelial adhesions in wild-type embryos (Figures 4A and 4D). In $Irf6^{+/-}$ embryos we detected bilateral oral adhesions at the tooth germ sites (Figure 4B). We also observed bilateral epithelial abnormalities in $Grhl3^{+/-}$ embryos (Figure 4E), but they differed from those seen in the $Irf6^{+/-}$ embryos in three respects. First, whereas oral adhesions in $Irf6^{+/-}$ embryos were more prominent at the tooth germ sites (Figure 4B), epithelial abnormalities in $Grhl3^{+/-}$ embryos were located throughout the oral cavity and most frequently posterior to the tooth germs (Figure 4E). Second, epithelial abnormalities included oral fusions (Figure 4E), which do not occur in $Irf6^{+/-}$ embryos. Here, we distinguish oral epithelial adhesions from oral fusions histologically. Whereas adhesions have a loss of periderm that allows cell interactions between two adjacent epithelial layers, fusions have a loss of both the periderm and the basal epithelial layers that allows cell interactions between the underlying mesenchymal cells from adjacent tissues. Finally, whereas oral adhesions in $Irf6^{+/-}$ occurred most frequently between the mandible and maxilla, oral fusions in $Grhl3^{+/-}$ embryos occurred between the mandible and either the palate or the maxilla. In the $Irf6^{+/-}$;$Grhl3^{+/-}$ double heterozygous embryos, we found oral adhesions at areas superficial to the tooth germ (Figure 4C), similar to $Irf6^{+/-}$ embryos, as well as oral adhesions and fusions posterior to the tooth germ (Figure 4F), similar to $Grhl3^{+/-}$ embryos. Thus, the oral histopathology of the $Irf6^{+/-}$;$Grhl3^{+/-}$ double heterozygote embryos provides no evidence for epistasis and suggests that *Irf6* and *Grhl3* function in independent but converging pathways during oral periderm development.

As previously observed in the single knockout $Irf6^{-/-}$ and $Grhl3^{-/-}$ embryos, we detected a reduction in

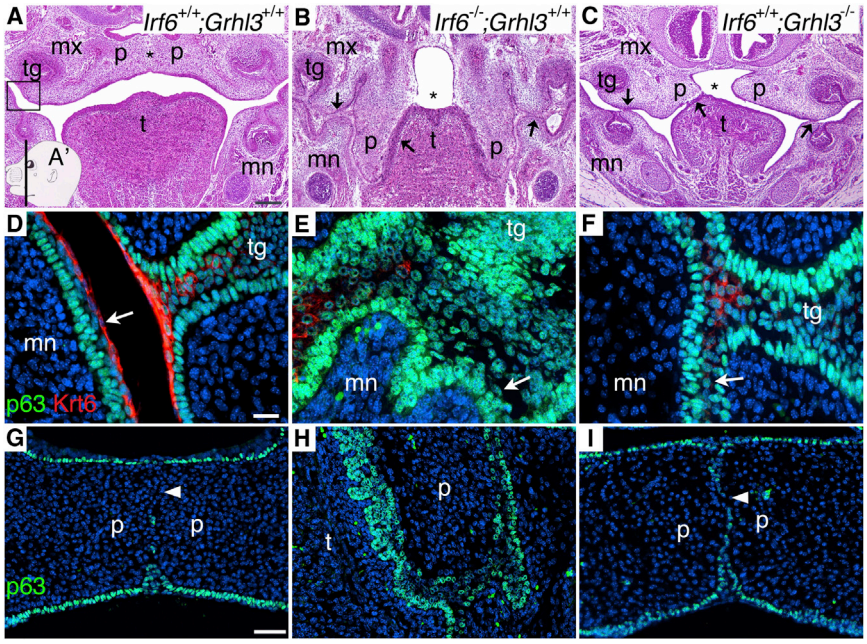

Figure 3. *Grhl3* Is Required for Murine Periderm and Palatal Development

(A–C) Haematoxylin and eosin staining of coronal sections of posterior palate at E15.5 (A′). Wild-type embryos showed complete fusion of palatal shelves (asterisk) (A). In contrast, *Irf6*$^{-/-}$ embryos have bilateral oral adhesions (arrows) and a fully penetrant cleft palate (asterisk) (B). Similarly, *Grhl3*$^{-/-}$ embryos have bilateral oral adhesions (arrows) (C). However, in *Grhl3*$^{-/-}$ embryos, adhesions were restricted to areas superficial to the tooth germ and palatal surfaces, and a cleft palate was observed in one of six embryos (asterisk) (C).

(D–F) Immunostaining for Krt6 (red) and p63 (green). Krt6 was expressed uniformly in the periderm superficial to the tooth germ (arrow) of wild-type embryos (D) (from boxed structure in A) but was very weakly expressed in *Irf6*$^{-/-}$ (E) and *Grhl3*$^{-/-}$ (F) embryos. p63 was expressed uniformly in the basal epithelium of wild-type (D) and *Grhl3*$^{-/-}$ (F) embryos but was expressed ectopically in suprabasal cells in *Irf6*$^{-/-}$ embryos (E).

(G–I) Loss of p63 expression marks normal dissolution of the medial edge epithelium (MEE) (arrowhead) in wild-type (G) and *Grhl3*$^{-/-}$ (I) embryos. In contrast, p63 expression persisted around the palatal epithelium in *Irf6*$^{-/-}$ embryos (H).

(D–I) Nuclei are counterstained with DAPI (blue).

Scale bars represent 2 mm for (A)–(C), 20 μm for (D)–(F), and 50 μm for (G)–(I). Labeled oral structures are mandible (mn), maxilla (mx), palatal shelf (p), tongue (t), and tooth germ (tg).

expression of Krt6 in both heterozygous embryos (Figure 4G versus 4H and 4I) and a more apparent reduction of Krt6 in the double heterozygous embryos (Figure 4J). At higher magnification, the loss in Krt6 staining coincided with the loss of oral periderm cells (Figure 4K versus 4L–4N). We did not detect any change in p63 expression in the *Irf6*$^{+/-}$ embryos (Figure 4O versus 4P). However, in the *Grhl3*$^{+/-}$ (Figure 4Q) and the *Irf6*$^{+/-}$;*Grhl3*$^{+/-}$ (Figure 4R) embryos, we observed a loss of expression of p63, indicating a loss of the basal epithelial cells at the sites of the oral fusions. Again, these molecular data suggest that *Irf6* and *Grhl3* function independently during palatal development.

Although we did not detect epistasis between *Irf6* and *Grhl3* during palatal development, we observed a 12% (6/51) rate of resorbing embryos (Table S3). This frequency was significantly higher than expected (3%, p value = 0.0008) for the C57BL/6 murine strain.[27] In addition, although we observed a Mendelian distribution of pups at birth (postnatal day 0, P0), *Irf6*$^{+/-}$;*Grhl3*$^{+/-}$ pups were significantly underrepresented at P21 (p value = 0.01). Thus, prenatal and postnatal lethality from crosses that generated the double heterozygous pups suggest positive epistasis between *Irf6* and *Grhl3* at other time points and/or tissues during development.

Discussion

By using a combination of whole-exome and Sanger sequencing methods, we identified mutations in *GRHL3* in eight families with VWS that had no causative mutations in *IRF6*, thus demonstrating that, when mutated, *GRHL3* is the gene responsible for VWS at the *VWS2* locus. Although previous studies had found *IRF6* mutations in 70% of families with VWS, there had been very little evidence for locus heterogeneity. Despite 15 published linkage studies on 49 families from throughout the world,[28] only one pedigree demonstrated linkage outside of the *IRF6* locus.[15] Because this family originated from Finland, a relatively isolated population, and because, at that time, only one member of the family had lip pits, the cardinal feature of VWS, the broader impact of this family on VWS genetics was uncertain. However, the finding of causative mutations in seven additional families from broad geographic and phenotypic spectra supports the clinical and biological significance of this locus for VWS and demonstrates that locus heterogeneity contributes to the genetic architecture of VWS.

The results from our mutation screen also suggest a complex allelic architecture for *GRHL3* in VWS. Based on the precedent of *IRF6*, we hypothesized that VWS resulting from mutation at the second locus (*VWS2*) would be caused by haploinsufficiency of *GRHL3*. Consistent with this hypothesis, we observed both missense and protein truncation mutations. In addition, the DECIPHER database (Database of Chromosomal Imbalance and Phenotype in Humans using Ensembl Resources)[29] includes a 1.9 Mb de novo deletion encompassing *GRHL3* in an individual with CP, club foot, developmental delay, prominent forehead, and a thin upper lip. In our small number of cases, we also observed a case of compound

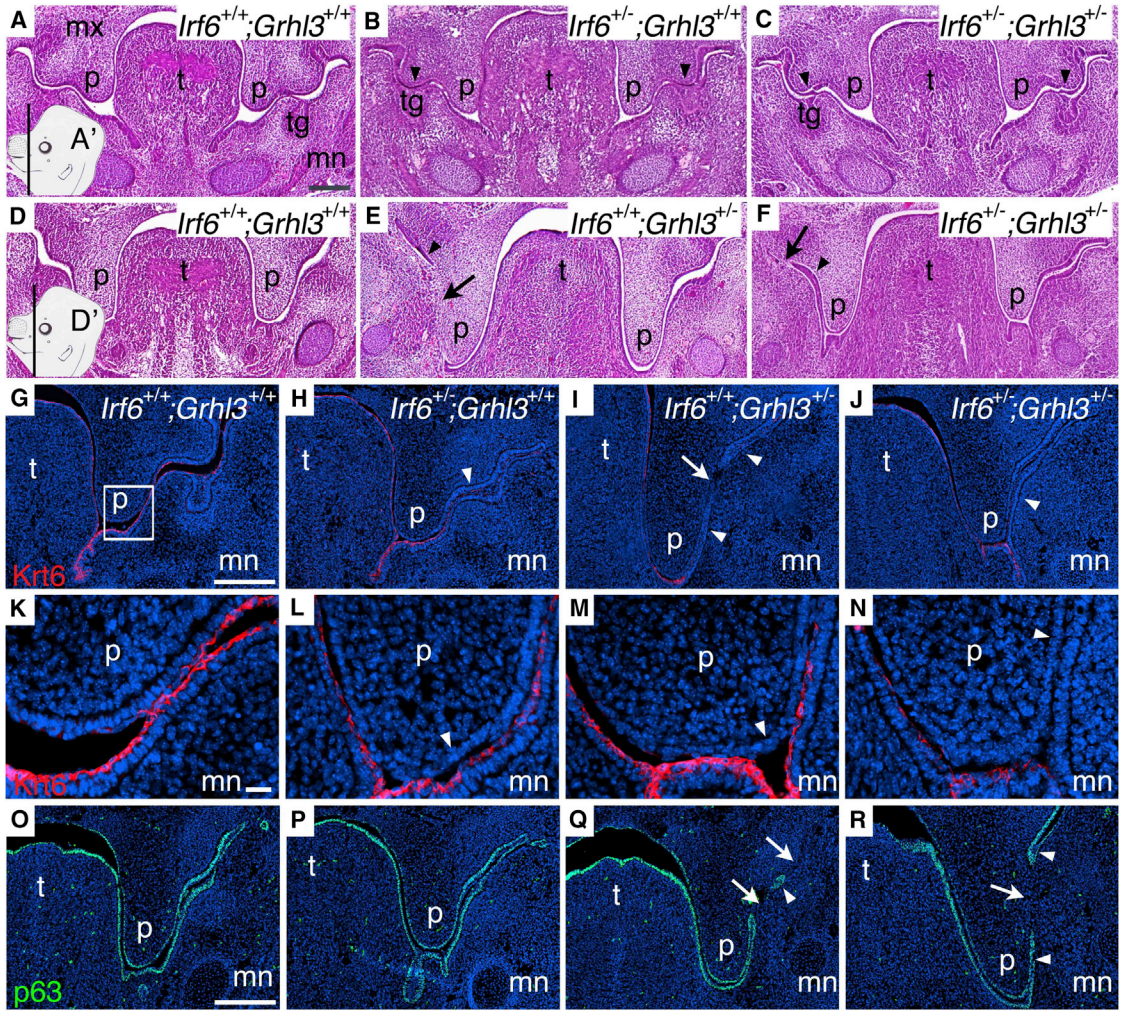

Figure 4. No Evidence for Genetic Interaction between *Irf6* and *Grhl3* in Murine Palatal Development

(A–F) Haematoxylin and eosin staining of coronal sections of E13.5 palate anterior (A') and posterior (D') to the tooth germ. Compared to wild-type embryos (A, D), $Irf6^{+/-}$ embryos had bilateral oral adhesions (arrowheads) at the tooth germ site (B). In contrast, $Grhl3^{+/-}$ littermates had oral adhesions (arrowheads) and fusions (arrow) located predominantly posterior to the tooth germ (E). $Irf6^{+/-}$;$Grhl3^{+/-}$ embryos (C, F) have oral adhesions (arrowheads) at the tooth germ (C) as well as adhesions (arrowheads) and fusions (arrow) posterior to the tooth germ (F).

(G–N) Krt6 immunostaining (red) of the oral periderm. Compared to wild-type embryos (G, enlarged in K), Krt6 expression in $Irf6^{+/-}$ (H, enlarged in L), $Grhl3^{+/-}$ (I, enlarged in M), and $Irf6^{+/-}$;$Grhl3^{+/-}$ (J, enlarged in N) embryos was markedly reduced along the oral surface of the palatal shelves and the mandible. Loss of Krt6 expression coincides with oral adhesions (arrowheads) and fusions (arrow).

(O–R) p63 immunostaining (green) of the basal epithelium was continuous in wild-type (O) and $Irf6^{+/-}$ (P) embryos. In contrast, p63 staining of $Grhl3^{+/-}$ (Q) and $Irf6^{+/-}$;$Grhl3^{+/-}$ (R) embryos was discontinuous. Oral fusions are seen between surfaces of the palate and mandible with mesenchymal communication (arrows) punctuating islands of p63-positive epithelial cells (arrowheads).

Scale bars represent 2 mm (A–F, G–J, and O–R) and 20 μm (K–N). Labeled oral structures are mandible (mn), maxilla (mx), palatal shelf (p), tongue (t), and tooth germ (tg).

heterozygous alleles for *GRHL3* (proband in VWS-III) and another case with a rare variant in both *IRF6* and *GRHL3* (proband in VWS-IV). However, all five *GRHL3* variants used in the zebrafish assay, including both alleles of the compound heterozygote individual, uniformally tested as dominant negative. If VWS-associated *GRHL3* alleles also have a dominant-negative effect in human tissues, it is not clear why they would be found in a coupled state, how the protein truncation alleles remain stable, and whether GRHL3 participates in protein complexes. Further genetic and biochemical studies will be required to understand the effects of these alleles in human tissues.

The analysis of human phenotypes suggests two clinical hypotheses. First, because individuals with *GRHL3* mutations were more likely to have CP and less likely to have CL/P than individuals with *IRF6* mutations, this association may be used to prioritize these two genes for mutation screens in VWS cases. We note that this association was made from a small number of individuals with *GRHL3* mutations ($n = 27$) and that nine individuals originated from one family (VWS-I). However, when we restricted the

analysis to a family-based phenotype (n = 8), we observed the same trends, although not achieving statistical significance because of low power. Second, like *IRF6*, common DNA variants in *GRHL3* may also be associated with isolated forms of orofacial clefting,[30] especially for CP, given the increased likelihood of CP in individuals with a mutation in *GRHL3*. However, multiple genome-wide association studies for CL/P[31] and one for CP[32] have not provided strong evidence for common variants at the *GRHL3* locus. Although these studies suggest that common DNA variants in *GRHL3* do not account for significant risk for CL/P or CP, *GRHL3* remains an excellent candidate gene for isolated orofacial clefts.

Finally, our analysis of phenotypes in *Irf6* and *Grhl3* mutant mice identified common and distinct oral abnormalities. Previous studies revealed that *Irf6* deficiency in mice could lead to an orofacial cleft by at least two pathophysiological mechanisms: abnormal periderm differentiation and failure of the medial edge epithelium (MEE) to dissolve.[11,33] The MEE was able to dissolve normally in embryos that lack *Grhl3*, so the common feature of *Irf6* and *Grhl3* mutants is failed periderm differentiation, strengthening the previously hypothesized role of periderm in development of the lip and palate.

In conclusion, these studies identify *GRHL3* as the second gene that when mutated leads to Van der Woude syndrome, thus confirming locus heterogeneity for this syndrome. Further, they strengthen the connection between cleft palate and abnormal periderm development. We anticipate that these findings will improve the molecular diagnostic for VWS and other forms of orofacial clefting.

Supplemental Data

Supplemental Data include three figures and three tables and can be found with this article online at http://www.cell.com/AJHG/.

Acknowledgments

We greatly appreciate the many individuals affected with VWS, their family members, and clinicians for participating in this study. We would like to thank Arianna L. Smith and Mager Scientific for technical assistance; Nicole Patel for the artistic renderings of murine embryos at E13.5 and E15.5; Päivi Lahermo for providing the Finnish controls and Pat Venta for critiques. Financial support for this research was provided by the Swedish Research Council 521-2007-3133 (M.P.-J.) and 2009-5091 (J.K.), by National Institutes of Health grants DE021071 (R.A.C.), DE13513 (B.C.S.), F31DE022696 (Y.A.K.), DE08559 (J.C.M.), GM008629 (E.J.L.), AR061586 (M.D.), and AR44882 (B.A.), and by the Sigrid Jusélius Foundation (J.K.).

Received: September 9, 2013
Accepted: November 14, 2013
Published: December 19, 2013

Web Resources

The URLs for data presented herein are as follows:

GATK, http://www.broadinstitute.org/gatk/

NHLBI Exome Sequencing Project (ESP) Exome Variant Server, http://evs.gs.washington.edu/EVS/

Online Mendelian Inheritance in Man (OMIM), http://www.omim.org/

Picard, http://picard.sourceforge.net/

Primer3, http://bioinfo.ut.ee/primer3-0.4.0/primer3/

UCSC Human Genome Browser, http://genome.ucsc.edu/cgi-bin/hgGateway

Accession Numbers

The dbSNP accession number for the *KTI12* (c.337_363delCCGA TCGCGGGACCTCAGGTGGCGGGC) variant reported in this paper is ss836732090.

References

1. Mace, K.A., Pearson, J.C., and McGinnis, W. (2005). An epidermal barrier wound repair pathway in *Drosophila* is mediated by grainy head. Science *308*, 381–385.
2. Ting, S.B., Caddy, J., Hislop, N., Wilanowski, T., Auden, A., Zhao, L.L., Ellis, S., Kaur, P., Uchida, Y., Holleran, W.M., et al. (2005). A homolog of *Drosophila* grainy head is essential for epidermal integrity in mice. Science *308*, 411–413.
3. Yu, Z., Lin, K.K., Bhandari, A., Spencer, J.A., Xu, X., Wang, N., Lu, Z., Gill, G.N., Roop, D.R., Wertz, P., and Andersen, B. (2006). The Grainyhead-like epithelial transactivator Get-1/Grhl3 regulates epidermal terminal differentiation and interacts functionally with LMO4. Dev. Biol. *299*, 122–136.
4. de la Garza, G., Schleiffarth, J.R., Dunnwald, M., Mankad, A., Weirather, J.L., Bonde, G., Butcher, S., Mansour, T.A., Kousa, Y.A., Fukazawa, C.F., et al. (2013). Interferon regulatory factor 6 promotes differentiation of the periderm by activating expression of Grainyhead-like 3. J. Invest. Dermatol. *133*, 68–77.
5. Sabel, J.L., d'Alençon, C., O'Brien, E.K., Van Otterloo, E., Lutz, K., Cuykendall, T.N., Schutte, B.C., Houston, D.W., and Cornell, R.A. (2009). Maternal Interferon Regulatory Factor 6 is required for the differentiation of primary superficial epithelia in *Danio* and *Xenopus* embryos. Dev. Biol. *325*, 249–262.
6. Botti, E., Spallone, G., Moretti, F., Marinari, B., Pinetti, V., Galanti, S., De Meo, P.D., De Nicola, F., Ganci, F., Castrignanò, T., et al. (2011). Developmental factor IRF6 exhibits tumor suppressor activity in squamous cell carcinomas. Proc. Natl. Acad. Sci. USA *108*, 13710–13715.
7. Tamura, T., Yanai, H., Savitsky, D., and Taniguchi, T. (2008). The IRF family transcription factors in immunity and oncogenesis. Annu. Rev. Immunol. *26*, 535–584.
8. Kondo, S., Schutte, B.C., Richardson, R.J., Bjork, B.C., Knight, A.S., Watanabe, Y., Howard, E., de Lima, R.L., Daack-Hirsch, S., Sander, A., et al. (2002). Mutations in IRF6 cause Van der Woude and popliteal pterygium syndromes. Nat. Genet. *32*, 285–289.
9. Ingraham, C.R., Kinoshita, A., Kondo, S., Yang, B., Sajan, S., Trout, K.J., Malik, M.I., Dunnwald, M., Goudy, S.L., Lovett, M., et al. (2006). Abnormal skin, limb and craniofacial morphogenesis in mice deficient for interferon regulatory factor 6 (Irf6). Nat. Genet. *38*, 1335–1340.
10. Richardson, R.J., Dixon, J., Malhotra, S., Hardman, M.J., Knowles, L., Boot-Handford, R.P., Shore, P., Whitmarsh, A., and Dixon, M.J. (2006). Irf6 is a key determinant of the keratinocyte proliferation-differentiation switch. Nat. Genet. *38*, 1329–1334.
11. Richardson, R.J., Dixon, J., Jiang, R., and Dixon, M.J. (2009). Integration of IRF6 and Jagged2 signalling is essential for

controlling palatal adhesion and fusion competence. Hum. Mol. Genet. *18*, 2632–2642.
12. Burdick, A.B., Bixler, D., and Puckett, C.L. (1985). Genetic analysis in families with van der Woude syndrome. J. Craniofac. Genet. Dev. Biol. *5*, 181–208.
13. de Lima, R.L., Hoper, S.A., Ghassibe, M., Cooper, M.E., Rorick, N.K., Kondo, S., Katz, L., Marazita, M.L., Compton, J., Bale, S., et al. (2009). Prevalence and nonrandom distribution of exonic mutations in interferon regulatory factor 6 in 307 families with Van der Woude syndrome and 37 families with popliteal pterygium syndrome. Genet. Med. *11*, 241–247.
14. Leslie, E.J., Standley, J., Compton, J., Bale, S., Schutte, B.C., and Murray, J.C. (2013). Comparative analysis of IRF6 variants in families with Van der Woude syndrome and popliteal pterygium syndrome using public whole-exome databases. Genet. Med. *15*, 338–344.
15. Koillinen, H., Wong, F.K., Rautio, J., Ollikainen, V., Karsten, A., Larson, O., Teh, B.T., Huggare, J., Lahermo, P., Larsson, C., and Kere, J. (2001). Mapping of the second locus for the Van der Woude syndrome to chromosome 1p34. Eur. J. Hum. Genet. *9*, 747–752.
16. Schutte, B.C., Bjork, B.C., Coppage, K.B., Malik, M.I., Gregory, S.G., Scott, D.J., Brentzell, L.M., Watanabe, Y., Dixon, M.J., and Murray, J.C. (2000). A preliminary gene map for the Van der Woude syndrome critical region derived from 900 kb of genomic sequence at 1q32-q41. Genome Res. *10*, 81–94.
17. Peyrard-Janvid, M., Pegelow, M., Koillinen, H., Larsson, C., Fransson, I., Rautio, J., Hukki, J., Larson, O., Karsten, A.L., and Kere, J. (2005). Novel and de novo mutations of the IRF6 gene detected in patients with Van der Woude or popliteal pterygium syndrome. Eur. J. Hum. Genet. *13*, 1261–1267.
18. Li, H., and Durbin, R. (2010). Fast and accurate long-read alignment with Burrows-Wheeler transform. Bioinformatics *26*, 589–595.
19. DePristo, M.A., Banks, E., Poplin, R., Garimella, K.V., Maguire, J.R., Hartl, C., Philippakis, A.A., del Angel, G., Rivas, M.A., Hanna, M., et al. (2011). A framework for variation discovery and genotyping using next-generation DNA sequencing data. Nat. Genet. *43*, 491–498.
20. McLaren, W., Pritchard, B., Rios, D., Chen, Y., Flicek, P., and Cunningham, F. (2010). Deriving the consequences of genomic variants with the Ensembl API and SNP Effect Predictor. Bioinformatics *26*, 2069–2070.
21. Pegelow, M., Koillinen, H., Magnusson, M., Fransson, I., Unneberg, P., Kere, J., Karsten, A., and Peyrard-Janvid, M. (2013). Association and mutation analyses of the IRF6 gene in families with non-syndromic and syndromic cleft lip and/or cleft palate. Cleft Palate Craniofac. J. Published online February 8, 2013. http://dx.doi.org/10.1597/11-220.
22. Thisse, C., and Thisse, B. (2008). High-resolution in situ hybridization to whole-mount zebrafish embryos. Nat. Protoc. *3*, 59–69.
23. Malik, S., Kakar, N., Hasnain, S., Ahmad, J., Wilcox, E.R., and Naz, S. (2010). Epidemiology of Van der Woude syndrome from mutational analyses in affected patients from Pakistan. Clin. Genet. *78*, 247–256.
24. Chalmers, A.D., Lachani, K., Shin, Y., Sherwood, V., Cho, K.W., and Papalopulu, N. (2006). Grainyhead-like 3, a transcription factor identified in a microarray screen, promotes the specification of the superficial layer of the embryonic epidermis. Mech. Dev. *123*, 702–718.
25. Mazzalupo, S., and Coulombe, P.A. (2001). A reporter transgene based on a human keratin 6 gene promoter is specifically expressed in the periderm of mouse embryos. Mech. Dev. *100*, 65–69.
26. Koster, M.I., Kim, S., Mills, A.A., DeMayo, F.J., and Roop, D.R. (2004). p63 is the molecular switch for initiation of an epithelial stratification program. Genes Dev. *18*, 126–131.
27. Krishnan, L., Guilbert, L.J., Wegmann, T.G., Belosevic, M., and Mosmann, T.R. (1996). T helper 1 response against *Leishmania major* in pregnant C57BL/6 mice increases implantation failure and fetal resorptions. Correlation with increased IFN-gamma and TNF and reduced IL-10 production by placental cells. J. Immunol. *156*, 653–662.
28. Schutte, B.C., Dixon, M.J., and Murray, J.C. (2008). IRF6 and the Van der Woude popliteal pterygium syndromes and the risk for non-syndromic cleft lip and palate. In Inborn Errors of Development, C. Epstein, ed. (New York: Oxford University Press), pp. 1069–1072.
29. Firth, H.V., Richards, S.M., Bevan, A.P., Clayton, S., Corpas, M., Rajan, D., Van Vooren, S., Moreau, Y., Pettett, R.M., and Carter, N.P. (2009). DECIPHER: Database of Chromosomal Imbalance and Phenotype in Humans Using Ensembl Resources. Am. J. Hum. Genet. *84*, 524–533.
30. Zucchero, T.M., Cooper, M.E., Maher, B.S., Daack-Hirsch, S., Nepomuceno, B., Ribeiro, L., Caprau, D., Christensen, K., Suzuki, Y., Machida, J., et al. (2004). Interferon regulatory factor 6 (IRF6) gene variants and the risk of isolated cleft lip or palate. N. Engl. J. Med. *351*, 769–780.
31. Ludwig, K.U., Mangold, E., Herms, S., Nowak, S., Reutter, H., Paul, A., Becker, J., Herberz, R., AlChawa, T., Nasser, E., et al. (2012). Genome-wide meta-analyses of nonsyndromic cleft lip with or without cleft palate identify six new risk loci. Nat. Genet. *44*, 968–971.
32. Beaty, T.H., Ruczinski, I., Murray, J.C., Marazita, M.L., Munger, R.G., Hetmanski, J.B., Murray, T., Redett, R.J., Fallin, M.D., Liang, K.Y., et al. (2011). Evidence for gene-environment interaction in a genome wide study of nonsyndromic cleft palate. Genet. Epidemiol. *35*, 469–478.
33. Knight, A.S., Schutte, B.C., Jiang, R., and Dixon, M.J. (2006). Developmental expression analysis of the mouse and chick orthologues of IRF6: the gene mutated in Van der Woude syndrome. Dev. Dyn. *235*, 1441–1447.